JACS
JOURNAL OF THE AMERICAN CHEMICAL SOCIETY
pubs.acs.org/JACS

Article

The Role of Torsion on the Force-Coupled Reactivity of a Fluorenyl Naphthopyran Mechanophore

Skylar K. Osler, Nathan A. Ballinger, and Maxwell J. Robb*

Cite This: J. Am. Chem. Soc. 2025, 147, 3904−3911

Read Online

ACCESS | Metrics & More | Article Recommendations | Supporting Information

ABSTRACT: The unique reactivity of molecules under force commands an understanding of structure−mechanochemical activity relationships. While conceptual frameworks for understanding force transduction in many systems are established, systematic investigations into force-coupled molecular torsions are limited. Here, we describe a novel fluorenyl naphthopyran mechanophore for which mechanical force is uniquely coupled to the torsional motions associated with the overall chemical transformation as a result of the conformational rigidity imposed by the fluorene group. Using a combined experimental and theoretical approach, we demonstrate that variation in the pulling geometry on the fluorene subunit results in significant differences in mechanochemical activity due to pronounced changes in how force is coupled to distinct torsional motions and their coherence with the nuclear motions that accompany the force-free ring-opening reaction. Notably, subtle changes in polymer attachment position lead to a >50% difference in the rate of mechanochemical activation in ultrasonication experiments. Our results offer new insights into the structural and geometric factors that influence mechanochemical reactivity by describing how mechanical force is coupled to a reaction that principally involves torsional motions.

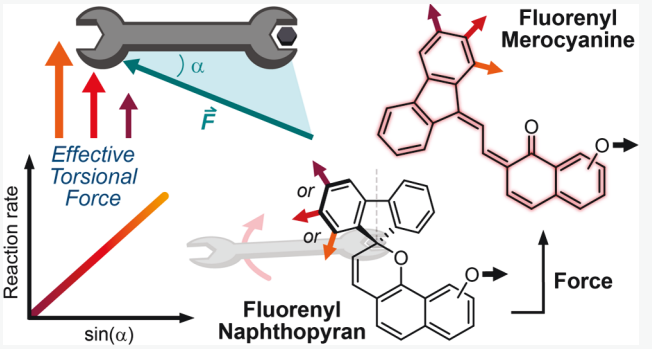

INTRODUCTION

Mechanophores are stress-sensitive molecules that undergo productive chemical transformations in response to mechanical force, which is transduced via covalently bound polymer chains.[1−3] Over the past two decades, a wide variety of mechanophores have been developed that can be harnessed to design force-responsive polymers and materials capable of myriad functions such as changes in color or luminescence,[4−7] small molecule release,[8−13] conductivity switching,[14,15] and catalysis.[16,17] Remarkably, the reaction pathways promoted by mechanical force often diverge from those under more conventional thermal or photochemical modes of activation.[18−20] Canonical examples include the mechanochemical ring-opening reactions of benzocyclobutene[21] and *gem*-dihalocyclopropanes,[22] which follow pathways that formally violate classical orbital symmetry rules.

The unique reactivity of molecules under the bias of mechanical force has inspired extensive investigations into structure−mechanochemical activity relationships.[23] At a fundamental level, mechanical force effectively reduces a reaction barrier by coupling mechanical work to the atomic motions inherent to the reaction coordinate.[24] Because force is a vector, the directional nature of mechanical force is a critical factor that influences reactivity. The regiochemistry[25−30] and stereochemistry[22,31] by which the polymers are connected to the mechanophore dictates the directionality of force transduction, and more specifically, how effectively mechanical force is coupled to elongation of the target scissile bond. Even relatively remote changes in the regiochemistry of polymer attachment on a diphenyl-substituted cyclobutane mechanophore were recently shown to significantly impact reactivity.[32] Likewise, a lever-arm effect associated with both polymer conformation[33] and the stereochemistry of alkene substituents adjacent to the mechanophore[34] reduces the force required for mechanochemical activation by increasing the efficiency of force transduction. A similar effect was implicated in the mechanochemical *cis*-to-*trans* isomerization of tetrahydrofuran-flanked C−C double bonds;[35] however, systematic investigations into force-coupled molecular rotations remain limited. For mechanophore reactions that principally involve rotational motions, we reasoned that effectively coupling external force to torsion would result in more efficient force transduction and greater mechanochemical reactivity.

Naphthopyran mechanophores undergo a ring-opening reaction under mechanical force to generate a colored merocyanine dye (Scheme 1a).[19] The tetrahedral carbon

Received: December 23, 2024
Revised: December 27, 2024
Accepted: December 30, 2024
Published: January 15, 2025

Scheme 1. Mechanically Activated Ring-Opening Reactions of (a) Typical Diaryl Naphthopyrans, and (b) a Conformationally Restricted Fluorenyl Naphthopyran

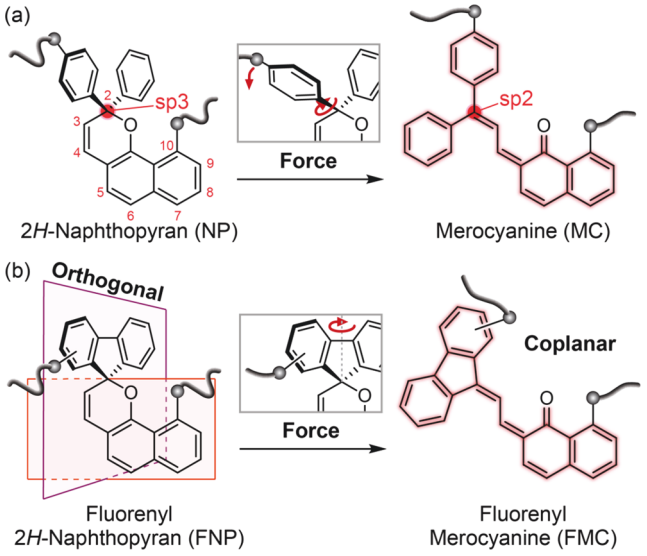

center of the pyran ring is typically substituted with two aryl groups, which are oriented perpendicular to the naphthalene core. The conversion of naphthopyran to the merocyanine product is accompanied by rehybridization at that position from Csp3 to Csp2. In effect, mechanical force causes a rotation at this diaryl-substituted carbon leading to a new coplanar arrangement in the merocyanine. However, modeling (and intuition) supports that the reaction actually proceeds with significant geometric distortion about the tetrahedral center. The regiochemistry of polymer attachment in archetypal naphthopyrans putatively influences force transduction to the scissile C−O pyran bond by controlling its alignment with the external force vector.[27] We hypothesized, however, that tethering the diaryl substituents at C2 in the form of a fluorene group would increase the conformational rigidity and enable more effective coupling of mechanical force to the torsional motion that accompanies the overall ring-opening reaction (Scheme 1b). Furthermore, we reasoned that varying the position of polymer attachment on the fluorene unit would modulate the degree to which mechanical force is coupled to this torsional motion, thereby leading to significant differences in reactivity.

RESULTS AND DISCUSSION

We identified three fluorenyl 2*H*-naphthopyran (FNP) structures with polymer attachment *via* an ester linkage at the 10-position and either the *ortho*, *meta*, or *para* position on the fluorene subunit with respect to the pyran ring (Figure 1a). We first sought to assess the relative mechanochemical reactivity of the three FNP congeners by performing density functional theory (DFT) calculations using the constrained geometries simulate external force (CoGEF) method on truncated models at the B3LYP/6-31G* level of theory (Figure 1b).[23,36] All three FNP regioisomers are predicted to undergo the anticipated ring-opening reaction upon mechanical elongation but at markedly different rupture forces (F_{max}), which span from a relatively low value of 3.7 nN for the *ortho*-FNP isomer to 4.9 nN for the *para*-FNP isomer (Figures 1c and S1−S3). A similar range of F_{max} values (1.1 nN) is predicted for the mechanochemical ring-opening reactions of an analogous series of FNP structures with polymer attachment *via* an ester linkage at the 9-position of the naphthopyran scaffold (Figures S4−S6). These results are consistent with the hypothesis that the position of polymer attachment on the fluorene group, rather than on the naphthalene core, differentiates reactivity. Notably, if the aryl substituents at C2 are not constrained by the biaryl bond, not only is a much smaller difference in reactivity predicted with values of F_{max} ranging from 4.1 to 4.5 nN, but the *para*-substituted compound is predicted to be the most reactive (Figures S7−S9).

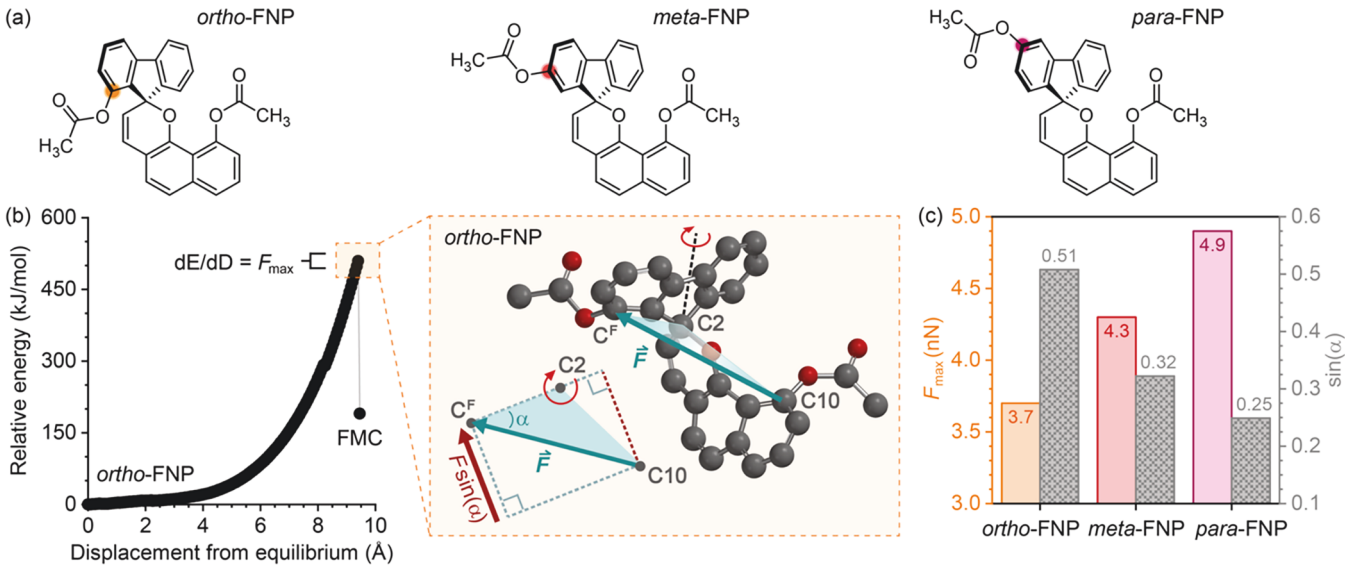

Figure 1. (a) Truncated models of fluorenyl naphthopyrans with polymer attachment at the *ortho*, *meta*, or *para* position on the fluorene subunit. (b) CoGEF calculations (B3LYP/6-31G*) were used to assess the relative reactivity of the fluorenyl naphthopyrans (representative data for the *ortho*-FNP congener shown). Angle α was determined from the computed structures immediately prior to C−O bond cleavage. (c) Relationship between predicted values of F_{max} and the effective torsional force as represented by the magnitude of sin(α).

https://doi.org/10.1021/jacs.4c18395
J. Am. Chem. Soc. 2025, 147, 3904−3911

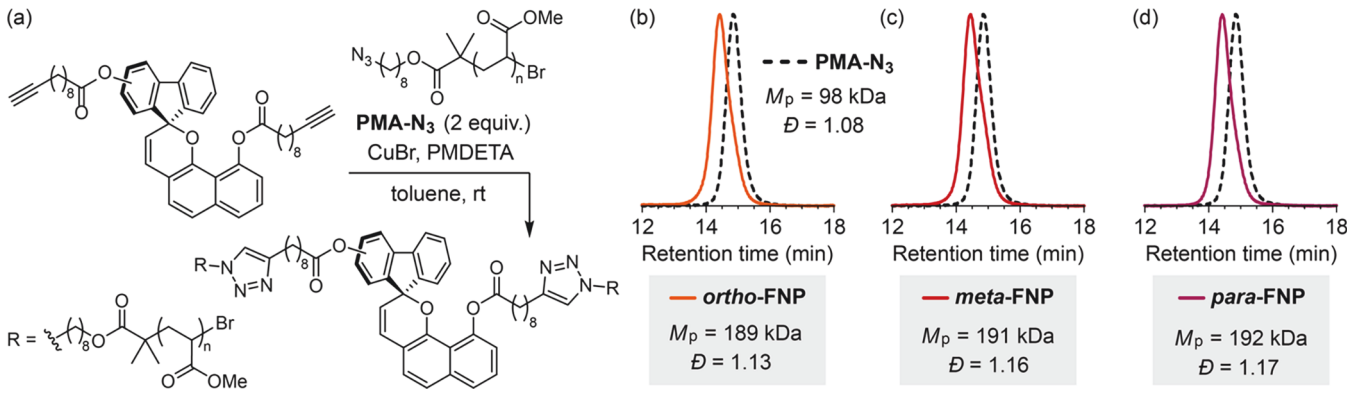

Figure 2. (a) Synthesis of poly(methyl acrylate) polymers containing a chain-centered FNP mechanophore via Cu-catalyzed azide−alkyne cycloaddition (CuAAC) "click" coupling. Characterization by GPC (RI response shown) confirms successful coupling reactions to generate chain-centered polymers (b) ***ortho*-FNP**, (c) ***meta*-FNP**, and (d) ***para*-FNP**.

To understand the differences in reactivity predicted for the FNP congeners, we examined the geometries of the computed structures from CoGEF calculations immediately prior to C−O bond cleavage to assess how changing the site of polymer attachment on the fluorene group influences mechanochemical coupling. In solid mechanics, the magnitude of the force that contributes to torque is equal to the component of the incident force vector in the plane of rotation perpendicular to the lever arm, or $F\sin(\alpha)$, as illustrated in Figure 1b.[37] In this case, the lever arm is defined by the line connecting C2 of the pyran ring and the carbon atom of the fluorene unit (C^F) bearing the ester group, which rotates in the plane defined by C2, C^F, and C10. Carbon atoms C10 and C^F were used to approximate the externally applied force vector (see SI for details).[27] This geometric analysis reveals that the effective torsional force scales linearly with the quantity $\sin(\alpha)$, which is strongly correlated with the trend in reactivity represented by the predicted values of F_{max} (Figure 1c). The progressively smaller values of $\sin(\alpha)$ for *ortho*, *meta*, and *para* substitution illustrate the diminishing proportion of the externally applied force that contributes effectively to torsion of the fluorene unit, thereby requiring correspondingly greater force applied to the molecule to achieve the ring-opening reaction. In particular, mechanical force is most efficiently coupled to rotation of the fluorene group in the *ortho*-FNP isomer, which is also expected to have the lowest activation barrier for merocyanine formation under force (*vide infra*). We note that a complete description of torque in this system would involve multiplying the quantity $F\sin(\alpha)$ by the length of the lever arm, r. Using the more complete geometric descriptor of $r{\cdot}\sin(\alpha)$ produces a similar trend as above with the predicted values of F_{max} (Figure S10). To further evaluate the generality of this method, we also performed a similar analysis on two different spiropyran mechanophores that are envisioned to undergo a rotational motion in their ring-opening reactions analogous to that of fluorenyl naphthopyrans.[26] We find that values of $\sin(\alpha)$, $r{\cdot}\sin(\alpha)$, and F_{max} are similarly correlated (Figure S11). Furthermore, the predicted trend in reactivity for the FNP congeners is inversely correlated with the degree of alignment between the external force vector and the pyran C−O bond (Figure S12). This observation further supports that the mechanochemical reactivity of fluorenyl naphthopyran is strongly influenced by force-coupled torsional motions rather than the extensional motions typically considered to drive reactivity in most mechanophores. We return to this idea with a more complete discussion below.

We next set out to experimentally investigate the relative mechanochemical reactivity of the FNP isomers using solution-phase ultrasonication.[1,38] Poly(methyl acrylate) (PMA) polymers ***ortho*-FNP**, ***meta*-FNP**, and ***para*-FNP** were prepared *via* a Cu(I)-catalyzed azide−alkyne cycloaddition (CuAAC) reaction between two equivalents of azide-terminated PMA (**PMA-N$_3$**, M_n = 89.3 kDa; M_p = 98.0 kDa; $Đ$ = 1.08) and the corresponding bis-alkyne-functionalized fluorenyl naphthopyrans (Figure 2, see SI for details). Importantly, this convergent synthetic strategy yields mechanophore chain-centered polymers with essentially identical molar mass and molar mass distribution, ensuring that uniform force is applied to each mechanophore during ultrasonication and enabling the direct comparison of mechanophore activation kinetics.[39]

Dilute solutions of ***ortho*-FNP**, ***meta*-FNP**, and ***para*-FNP** (2 mg/mL in THF, 30 mM BHT) were subjected to pulsed ultrasonication (−70 ± 5 °C, 1 s on/3 s off, 20 kHz, 6.5 ± 0.1 W cm^{-2}) for 90 min ("on" time) and aliquots were periodically removed for characterization by ultraviolet−visible (UV−vis) absorption spectroscopy to measure merocyanine accumulation (Figures 3a,b and S13). Ultrasound-induced mechanochemical activation of the FNP-containing polymers is expected to generate a persistent merocyanine dye *via* scission of the naphthyl C(O)−O ester bond that accompanies the ring-opening reaction, as observed previously for related naphthopyran scaffolds.[40,41] Nevertheless, we also verified that thermal reversion of the merocyanine dye containing an intact ester group does not occur at these low temperatures, thus guaranteeing the irreversible accumulation of all possible merocyanine products in the sonication experiments (Figure S14). The absorption spectra of the mechanochemical reaction products are unchanged 90 min after sonication, further confirming that no merocyanine reversion occurs under the experimental conditions (Figures 3b and S13). Finally, the absorption spectra obtained upon mechanochemical activation of ***ortho*-FNP**, ***meta*-FNP**, and ***para*-FNP** closely match the spectra of independently prepared small molecule model compounds, indicating that each FNP mechanophore produces the anticipated merocyanine dye (Figure S15).

The rate of mechanochemical merocyanine formation for each mechanophore was determined by fitting the time-dependent absorbance values at the observed λ_{max} to an

https://doi.org/10.1021/jacs.4c18395
J. Am. Chem. Soc. 2025, 147, 3904−3911

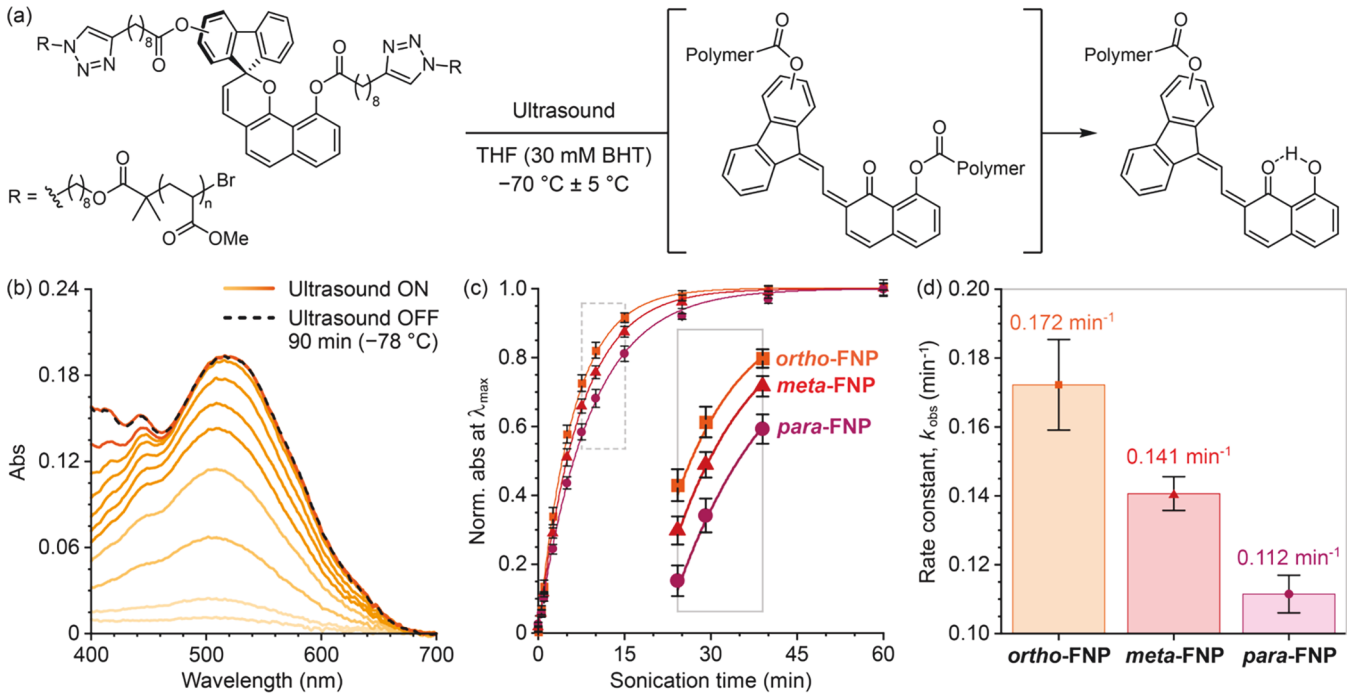

Figure 3. (a) Ultrasound-induced mechanochemical activation of fluorenyl naphthopyrans results in a ring-opening reaction and ester scission to generate a permanent merocyanine dye. (b) Representative UV−vis absorption spectra acquired during and after the sonication of ***ortho*-FNP**. (c) Absorbance monitored at λ_{max} as a function of sonication time for ***ortho*-PMA** (510 nm), ***meta*-PMA** (520 nm), and ***para*-PMA** (525 nm) fit to first-order kinetics and normalized to the plateau value. Data points and error bars represent average values and standard deviation from 3−4 replicate trials. (d) Rate constants (k_{obs}) for merocyanine accumulation determined from the data in (c).

expression of simple first-order kinetics (Figure 3c, see SI for details). Average values of the observed rate constant, k_{obs}, for each mechanophore were determined from 3−4 replicate trials (Figure 3d). The relative rate of merocyanine formation follows the order ***ortho*-FNP** (most reactive) > ***meta*-FNP** > ***para*-FNP** (least reactive), in agreement with the trend predicted from CoGEF calculations. Analysis using an unpaired *t* test confirms that the differences in the measured rate constants are statistically significant ($p < 0.05$). Control experiments also confirm that the observed kinetics are not convoluted by either the secondary ester scission reaction or variation in the rate of nonspecific backbone scission. Reaction rates for an analogous series of FNP mechanophores with polymer attachment at the 9-position of the naphthopyran, which do not undergo ester scission to generate a persistent merocyanine,[40,41] follow the same trend as above with rate constants for the *ortho*- and *para*-substituted mechanophores closely matching those of ***ortho*-FNP** and ***para*-FNP**, respectively, while the *meta*-substituted mechanophore reacts at an intermediate rate (Figures S16−S18). Notably, k_{obs} represents the sum of the rate constants for mechanophore activation and nonspecific backbone scission, which is always a competing pathway.[42,43] GPC measurements further confirmed that the rate of nonspecific backbone scission is invariant with changes in the attachment geometry on the fluorene group (Figure S19, see SI for details). Mechanochemical activation rates were also determined for another series of polymers with $M_n \sim 150$ kDa incorporating chain-centered *ortho*-FNP, *meta*-FNP, and *para*-FNP mechanophores, revealing the same trend in reactivity with average values of k_{obs} of 0.128, 0.107, and 0.082 min^{-1}, respectively (Figure S20, see SI for details). These results further support that the significant differences in mechanochemical activity for the regioisomeric FNP mechanophores are conserved across different batches of polymers and for polymers of substantially different molar mass.

To better understand the impact of polymer attachment position on the mechanochemical reactivity of the FNP mechanophore system, we consider the changes in molecular geometry associated with the force-free ring-opening reaction that are distinct from the rotational motions considered previously (Figure 4). Progression from the equilibrium geometry of fluorenyl naphthopyran to the force-free transition state is accompanied by a significant increase (+32°) in the angle γ defined by a line that bisects the fluorene group and the C2−C3 bond (Figure 4a). Ring opening of the pyran is accompanied by rehybridization of C2 from Csp3 to Csp2, which causes an increase in angle γ approaching 180° in the merocyanine product. Interestingly, CoGEF calculations predict this same torsional motion to be well-coupled to mechanical elongation of the *ortho*-FNP mechanophore; γ is similarly increased by 33° in the structure immediately prior to C−O bond cleavage relative to the starting material (Figures 4b and S21). In contrast, only a slight increase in γ of 7° is observed for the *meta*-FNP analogue, while mechanical elongation of the *para*-FNP model actually decreases γ from 127 to 113° prior to bond rupture. The correlation between the rate of mechanophore activation and $\Delta\gamma$ suggests that the pulling geometry not only dictates the efficiency with which mechanical force is coupled to the rotation of the fluorene group as described earlier, but secondary structural effects[44−46] strongly influence the coherence with which the torsional motions under applied tension mimic the natural nuclear motions associated with the ring-opening reaction and thus mechanochemical coupling. We note that similar secondary structural effects from rehybridization have been previously

https://doi.org/10.1021/jacs.4c18395
J. Am. Chem. Soc. 2025, 147, 3904−3911

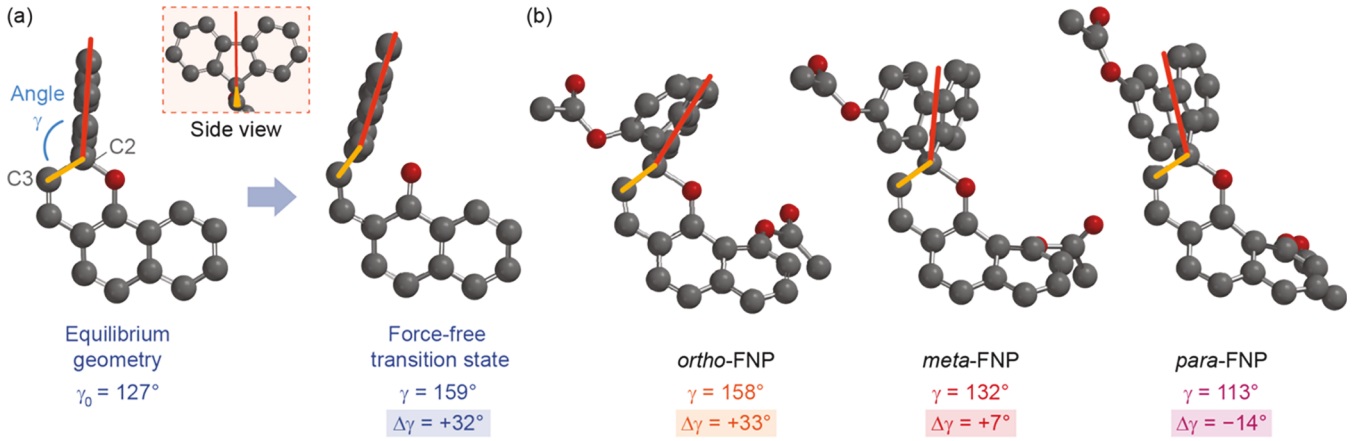

Figure 4. (a) Optimized geometries calculated by DFT for unsubstituted fluorenyl naphthopyran and the force-free transition state structure (B3LYP/6-31G*). (b) Truncated models *ortho*-FNP, *meta*-FNP, and *para*-FNP from CoGEF calculations immediately prior to C−O bond cleavage. The angle γ is defined by a line bisecting the fluorene group and the bond between carbon centers C2 and C3.

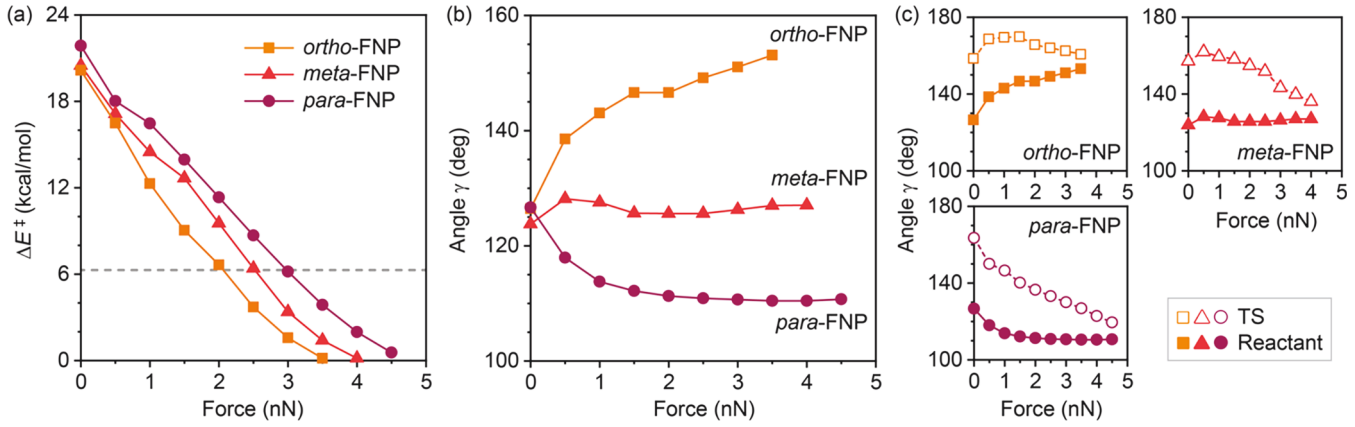

Figure 5. (a) Calculated barrier height ($\Delta E^{\ddagger}$) for naphthopyran ring opening as a function of applied force from EFEI calculations (uB3LYP-D3BJ/def2-TZVPP). The dashed gray line represents the activation barrier (6.3 kcal/mol) below which the thermal ring-opening reaction is expected to occur rapidly at −70 °C. (b) Angle γ in each fluorenyl naphthopyran congener, and (c) comparison of angle γ between the transition state (TS) and reactant structures as a function of applied force.

reported by Craig and co-workers to describe the mechanochemical dissociation of phenyl benzyl ether, for example, which is less labile than expected due to an overall molecular contraction that occurs during C−O bond elongation that is poorly coupled to an applied force of tension.[44]

The structures obtained from CoGEF calculations immediately prior to C−O bond cleavage offer a compelling snapshot of the mechanochemical reaction, but fail to quantitatively describe the energetic and geometric changes that occur over the relevant range of forces. Therefore, we performed DFT calculations using the external force is explicitly included (EFEI) method[47,48] on the same truncated models used in the CoGEF calculations to quantify how the reaction barriers and molecular geometries, including angle γ, evolve as a function of external force (Figure 5, see SI for details). In agreement with the experimental kinetic data and CoGEF calculations, the EFEI calculations predict that the barrier ($\Delta E^{\ddagger}$) of the naphthopyran ring-opening reaction is lowest for *ortho*-FNP and highest for *para*-FNP at all forces (Figure 5a). The dashed gray line in Figure 5a represents the activation barrier (6.3 kcal/mol) below which the thermal ring-opening reaction is expected to occur rapidly on the microsecond time scale of cavitation-induced chain extension during ultrasonication at −70 °C (see SI for details).[38,49] At this threshold of $\Delta E^{\ddagger}$, the ring-opening reaction requires approximately 2.1, 2.5, and 3.0 nN of force for *ortho*-FNP, *meta*-FNP, and *para*-FNP, respectively. Thus, the calculated barriers support that the mechanochemical reactivity of FNP mechanophores follows the order *ortho*-FNP > *meta*-FNP > *para*-FNP consistent with the experimental observations and CoGEF calculations.

To confirm that the secondary structural effects involving the torsional motion of the fluorene group illustrated in Figure 4 are not merely a consequence of varying degrees of distortion at different forces resulting from changes in the pulling geometry, we examined how angle γ evolves as a function of applied force in structures from the EFEI calculations (Figure 5b). At low force (0.5 nN), a sharp increase in angle γ from 126 to 139° is observed for *ortho*-FNP, which continues to increase toward linearity reaching 153° at 3.5 nN of applied force. This trend is consistent with the CoGEF predictions described above and replicates the geometric changes associated with the expected rehybridization at C2 from Csp^3 to Csp^2 that accompanies the naphthopyran ring-opening reaction. In contrast, only a small increase in angle γ of 4° is observed for *meta*-FNP at 0.5 nN, and γ remains relatively constant across the range of forces studied up to 4 nN. For *para*-FNP, angle γ decreases from 127 to 118° at 0.5 nN and steadily reaches a minimum of 110° at 4.5 nN of applied force.

https://doi.org/10.1021/jacs.4c18395
J. Am. Chem. Soc. 2025, 147, 3904−3911

Again, the force-induced nuclear distortions of *para*-FNP oppose the natural torsional motions of the fluorene group that accompany rehybridization at C2. These observations strongly support the results from CoGEF calculations above and confirm that the highly differentiated changes in reactant geometry for each FNP congener are evident across the entire range of relevant forces.

Results of the EFEI calculations also provide further insight into the force-modified potential energy surface by illustrating how the transition state geometries of the FNP mechanophores evolve relative to the reactant structures as a function of applied force (Figure 5c). Similar to the transition state structure of the unsubstituted fluorenyl naphthopyran model illustrated in Figure 4a, angle γ is approximately 160° in the force-free transition state structure of each FNP regioisomer. Upon increasing the applied force from 0.5 to 4.5 nN, the difference in angle γ between respective reactant and transition state structures decreases as the transition state geometries become more "reactant-like".[25] That is, consistent with Hammond's postulate, angle γ converges as the reactant and transition state structures of each FNP mechanophore become exceedingly similar upon lowering the reaction barrier with increasing applied force; the force at which angle γ converges reflects the relative mechanochemical activity of each FNP congener. This convergent behavior further supports that the changes in angle γ describe a motion that is coupled to the naphthopyran ring-opening reaction.

Finally, we sought to further understand the importance of torsion by examining other factors that may contribute to the force-coupled reactivity of fluorenyl naphthopyran mechanophores. Using structures from the EFEI calculations, we interrogated alternative molecular motions including torsion of the pyran ring as well as the naphthalene core; however, these molecular distortions are poorly coupled to either external force or the natural atomic motions accompanying the thermal ring-opening reaction, respectively (Figures S22−S23). We further examined the FNP mechanophores in the context of other popular methods for describing mechanochemical coupling. As mentioned above, force vector alignment analysis[27] reveals that *para*-FNP exhibits the best alignment between the external force vector and the labile C−O bond while *ortho*-FNP exhibits the poorest alignment (see Figure S12). While only qualitative, this trend is nevertheless in direct contrast to the theoretically predicted and experimentally observed relative reactivities of the FNP mechanophores and suggests that the externally applied force is not directly coupled to the elongation and rupture of the C−O pyran bond to induce the ring-opening reaction. Activation length ($\Delta x^{\ddagger}$) is a more quantitative descriptor of mechanochemical coupling[24] that has been used extensively to describe the relative activity of various mechanophores including *gem*-dihalocyclopropanes,[33,34] benzocyclobutenes,[50] spiropyrans,[26] and furan−maleimide Diels−Alder adducts.[51] The activation length reflects the extension in the transition state relative to the reactant structure projected along the external force vector. For reactions with similar force-free activation energies, such as the case of the FNP mechanophores, a transformation that is better coupled to a force of tension would be expected to have a larger value of $\Delta x^{\ddagger}$ and exhibit a faster rate of reaction at a given force or under similar experimental conditions. Notably, activation length analysis reveals similar values of $\Delta x^{\ddagger}$ for *ortho*-FNP, *meta*-FNP, and *para*-FNP (0.57, 0.45, and 0.45 Å, respectively) despite the significant differences in measured mechanochemical activation rates (Figure S24, see SI for details). In particular, the identical values of $\Delta x^{\ddagger}$ for *meta*-FNP and *para*-FNP strongly suggests that mechanochemical coupling does not arise from the direct elongational activation of the C−O pyran bond for the fluorenyl naphthopyran mechanophores. Taken together, the inconsistency of these models with the theoretically predicted and experimentally determined activities of the fluorenyl naphthopyran mechanophores further supports that mechanochemical reactivity in this system is differentiated by changes in force-coupled torsional motions distinct from more conventional frameworks for describing mechanochemical coupling.

CONCLUSIONS

In summary, we describe the mechanochemical reactivity of a series of regioisomeric fluorenyl naphthopyran mechanophores. Unlike typical diaryl naphthopyrans, the conformational rigidity of the fluorene group enforces well-defined torsional motions in the ring-opening reaction leading to the merocyanine product. Our results demonstrate that the efficiency with which external force is coupled to the rotation of the fluorene unit varies systematically depending on the position of polymer attachment. Moreover, variation in pulling geometry is shown to significantly impact the torsional motion of the fluorene group with respect to its coherence with the natural nuclear motions associated with the force-free ring-opening reaction. These aspects are fundamental in dictating mechanochemical coupling, and therefore the relative mechanochemical reactivity of the fluorenyl naphthopyran mechanophores. This study offers new insights into the structural features that govern mechanochemical reactions and, in particular, how mechanical work is coupled to chemical transformations that principally involve torsional motions.

ASSOCIATED CONTENT

Supporting Information

The Supporting Information is available free of charge at https://pubs.acs.org/doi/10.1021/jacs.4c18395.

Experimental details, synthetic procedures, DFT calculations, GPC chromatograms, UV−vis absorption data, and NMR spectra (PDF)

XYZ coordinates for computed structures (ZIP)

AUTHOR INFORMATION

Corresponding Author

Maxwell J. Robb − *Division of Chemistry and Chemical Engineering, California Institute of Technology, Pasadena, California 91125, United States;* orcid.org/0000-0002-0528-9857; Email: mrobb@caltech.edu

Authors

Skylar K. Osler − *Division of Chemistry and Chemical Engineering, California Institute of Technology, Pasadena, California 91125, United States;* orcid.org/0000-0003-1021-7011

Nathan A. Ballinger − *Division of Chemistry and Chemical Engineering, California Institute of Technology, Pasadena, California 91125, United States;* orcid.org/0000-0002-9213-529X

Complete contact information is available at: https://pubs.acs.org/10.1021/jacs.4c18395

https://doi.org/10.1021/jacs.4c18395
J. Am. Chem. Soc. 2025, 147, 3904−3911

Notes

The authors declare no competing financial interest.

■ ACKNOWLEDGMENTS

Financial support from an NSF CAREER award (CHE-2145791) and the Rose Hills Foundation Innovator Award is gratefully acknowledged. We thank Molly E. McFadden, Soren Holm, and Ilia Kevlishvili for helpful discussions. We thank the Center for Catalysis and Chemical Synthesis of the Beckman Institute at Caltech for access to equipment and the Resnick High Performance Computing Center, a facility supported by Resnick Sustainability Institute at Caltech. M.J.R. gratefully acknowledges the Alfred P. Sloan Foundation for a Sloan Research Fellowship and the Camille and Henry Dreyfus Foundation for a Camille Dreyfus Teacher-Scholar Award.

■ REFERENCES

(1) Li, J.; Nagamani, C.; Moore, J. S. Polymer Mechanochemistry: From Destructive to Productive. *Acc. Chem. Res.* **2015**, *48*, 2181−2190.
(2) Beyer, M. K.; Clausen-Schaumann, H. Mechanochemistry: The Mechanical Activation of Covalent Bonds. *Chem. Rev.* **2005**, *105*, 2921−2948.
(3) Caruso, M. M.; Davis, D. A.; Shen, Q.; Odom, S. A.; Sottos, N. R.; White, S. R.; Moore, J. S. Mechanically-Induced Chemical Changes in Polymeric Materials. *Chem. Rev.* **2009**, *109*, 5755−5798.
(4) Davis, D. A.; Hamilton, A.; Yang, J.; Cremar, L. D.; Van Gough, D.; Potisek, S. L.; Ong, M. T.; Braun, P. V.; Martínez, T. J.; White, S. R.; Moore, J. S.; Sottos, N. R. Force-induced activation of covalent bonds in mechanoresponsive polymeric materials. *Nature* **2009**, *459*, 68−72.
(5) Göstl, R.; Sijbesma, R. P. π-extended anthracenes as sensitive probes for mechanical stress. *Chem. Sci.* **2016**, *7*, 370−375.
(6) Chen, Y.; Spiering, A. J. H.; Karthikeyan, S.; Peters, G. W. M.; Meijer, E. W.; Sijbesma, R. P. Mechanically induced chemiluminescence from polymers incorporating a 1,2-dioxetane unit in the main chain. *Nat. Chem.* **2012**, *4*, 559−562.
(7) Liu, P.; Tseng, Y.-L.; Ge, L.; Zeng, T.; Shabat, D.; Robb, M. J. Mechanically Triggered Bright Chemiluminescence from Polymers by Exploiting a Synergy between Masked 2-Furylcarbinol Mechanophores and 1,2-Dioxetane Chemiluminophores. *J. Am. Chem. Soc.* **2024**, *146*, 22151−22156.
(8) Diesendruck, C. E.; Steinberg, B. D.; Sugai, N.; Silberstein, M. N.; Sottos, N. R.; White, S. R.; Braun, P. V.; Moore, J. S. Proton-Coupled Mechanochemical Transduction: A Mechanogenerated Acid. *J. Am. Chem. Soc.* **2012**, *134*, 12446−12449.
(9) Larsen, M. B.; Boydston, A. J. Flex-Activated" Mechanophores: Using Polymer Mechanochemistry To Direct Bond Bending Activation. *J. Am. Chem. Soc.* **2013**, *135*, 8189−8192.
(10) Hu, X.; Zeng, T.; Husic, C. C.; Robb, M. J. Mechanically Triggered Small Molecule Release from a Masked Furfuryl Carbonate. *J. Am. Chem. Soc.* **2019**, *141*, 15018−15023.
(11) Shi, Z.; Song, Q.; Göstl, R.; Herrmann, A. Mechanochemical activation of disulfide-based multifunctional polymers for theranostic drug release. *Chem. Sci.* **2021**, *12*, 1668−1674.
(12) Sun, Y.; Neary, W. J.; Burke, Z. P.; Qian, H.; Zhu, L.; Moore, J. S. Mechanically Triggered Carbon Monoxide Release with Turn-On Aggregation-Induced Emission. *J. Am. Chem. Soc.* **2022**, *144*, 1125−1129.
(13) Zeng, T.; Ordner, L. A.; Liu, P.; Robb, M. J. Multi-mechanophore Polymers for Mechanically Triggered Small Molecule Release with Ultrahigh Payload Capacity. *J. Am. Chem. Soc.* **2024**, *146*, 95−100.
(14) Chen, Z.; Mercer, J. A. M.; Zhu, X.; Romaniuk, J. A. H.; Pfattner, R.; Cegelski, L.; Martinez, T. J.; Burns, N. Z.; Xia, Y. Mechanochemical unzipping of insulating polyladderene to semiconducting polyacetylene. *Science* **2017**, *357*, 475−479.
(15) Boswell, B. R.; Mansson, C. M. F.; Cox, J. M.; Jin, Z.; Romaniuk, J. A. H.; Lindquist, K. P.; Cegelski, L.; Xia, Y.; Lopez, S. A.; Burns, N. Z. Mechanochemical synthesis of an elusive fluorinated polyacetylene. *Nat. Chem.* **2021**, *13*, 41−46.
(16) Piermattei, A.; Karthikeyan, S.; Sijbesma, R. P. Activating catalysts with mechanical force. *Nat. Chem.* **2009**, *1*, 133−137.
(17) Michael, P.; Binder, W. H. A Mechanochemically Triggered "Click" Catalyst. *Angew. Chem., Int. Ed.* **2015**, *54*, 13918−13922.
(18) Nixon, R.; De Bo, G. Three concomitant C−C dissociation pathways during the mechanical activation of an N-heterocyclic carbene precursor. *Nat. Chem.* **2020**, *12*, 826−831.
(19) McFadden, M. E.; Barber, R. W.; Overholts, A. C.; Robb, M. J. Naphthopyran molecular switches and their emergent mechanochemical reactivity. *Chem. Sci.* **2023**, *14*, 10041−10067.
(20) Liu, Y.; Holm, S.; Meisner, J.; Jia, Y.; Wu, Q.; Woods, T. J.; Martinez, T. J.; Moore, J. S. Flyby reaction trajectories: Chemical dynamics under extrinsic force. *Science* **2021**, *373*, 208−212.
(21) Hickenboth, C. R.; Moore, J. S.; White, S. R.; Sottos, N. R.; Baudry, J.; Wilson, S. R. Biasing reaction pathways with mechanical force. *Nature* **2007**, *446*, 423−427.
(22) Wang, J.; Kouznetsova, T. B.; Niu, Z.; Ong, M. T.; Klukovich, H. M.; Rheingold, A. L.; Martinez, T. J.; Craig, S. L. Inducing and quantifying forbidden reactivity with single-molecule polymer mechanochemistry. *Nat. Chem.* **2015**, *7*, 323−327.
(23) Klein, I. M.; Husic, C. C.; Kovács, D. P.; Choquette, N. J.; Robb, M. J. Validation of the CoGEF Method as a Predictive Tool for Polymer Mechanochemistry. *J. Am. Chem. Soc.* **2020**, *142*, 16364−16381.
(24) Brown, C. L.; Craig, S. L. Molecular engineering of mechanophore activity for stress-responsive polymeric materials. *Chem. Sci.* **2015**, *6*, 2158−2165.
(25) Konda, S. S. M.; Brantley, J. N.; Varghese, B. T.; Wiggins, K. M.; Bielawski, C. W.; Makarov, D. E. Molecular Catch Bonds and the Anti-Hammond Effect in Polymer Mechanochemistry. *J. Am. Chem. Soc.* **2013**, *135*, 12722−12729.
(26) Gossweiler, G. R.; Kouznetsova, T. B.; Craig, S. L. Force-Rate Characterization of Two Spiropyran-Based Molecular Force Probes. *J. Am. Chem. Soc.* **2015**, *137*, 6148−6151.
(27) Robb, M. J.; Kim, T. A.; Halmes, A. J.; White, S. R.; Sottos, N. R.; Moore, J. S. Regioisomer-Specific Mechanochromism of Naphthopyran in Polymeric Materials. *J. Am. Chem. Soc.* **2016**, *138*, 12328−12331.
(28) Stevenson, R.; De Bo, G. Controlling Reactivity by Geometry in Retro-Diels−Alder Reactions under Tension. *J. Am. Chem. Soc.* **2017**, *139*, 16768−16771.
(29) Wang, L.; Zheng, X.; Kouznetsova, T. B.; Yen, T.; Ouchi, T.; Brown, C. L.; Craig, S. L. Mechanochemistry of Cubane. *J. Am. Chem. Soc.* **2022**, *144*, 22865−22869.
(30) Ding, S.; Wang, W.; Germann, A.; Wei, Y.; Du, T.; Meisner, J.; Zhu, R.; Liu, Y. Bicyclo[2.2.0]hexene: A Multicyclic Mechanophore with Reactivity Diversified by External Forces. *J. Am. Chem. Soc.* **2024**, *146*, 6104−6113.
(31) Kryger, M. J.; Munaretto, A. M.; Moore, J. S. Structure−Mechanochemical Activity Relationships for Cyclobutane Mechanophores. *J. Am. Chem. Soc.* **2011**, *133*, 18992−18998.
(32) Flear, E. J.; Horst, M.; Yang, J.; Xia, Y. Force Transduction Through Distant Force-Bearing Regioisomeric Linkages Affects the Mechanochemical Reactivity of Cyclobutane. *Angew. Chem., Int. Ed.* **2024**, *63*, No. e202406103.
(33) Klukovich, H. M.; Kouznetsova, T. B.; Kean, Z. S.; Lenhardt, J. M.; Craig, S. L. A backbone lever-arm effect enhances polymer mechanochemistry. *Nat. Chem.* **2013**, *5*, 110−114.
(34) Wang, J.; Kouznetsova, T. B.; Kean, Z. S.; Fan, L.; Mar, B. D.; Martínez, T. J.; Craig, S. L. A Remote Stereochemical Lever Arm Effect in Polymer Mechanochemistry. *J. Am. Chem. Soc.* **2014**, *136*, 15162−15165.
(35) Huang, W.; Zhu, Z.; Wen, J.; Wang, X.; Qin, M.; Cao, Y.; Ma, H.; Wang, W. Single Molecule Study of Force-Induced Rotation of

https://doi.org/10.1021/jacs.4c18395
J. Am. Chem. Soc. 2025, 147, 3904−3911

Carbon−Carbon Double Bonds in Polymers. *ACS Nano* **2017**, *11*, 194−203.
(36) Beyer, M. K. The mechanical strength of a covalent bond calculated by density functional theory. *J. Chem. Phys.* **2000**, *112*, 7307−7312.
(37) Young, H. D.; Zemansky, M. W.; Sears, F. W.; Freedman, R. A.; Ford, A. L. *Sears & Zemansky's University Physics with Modern Physics*, 15th ed.; Pearson: Harlow, Essex, 2020.
(38) May, P. A.; Moore, J. S. Polymer mechanochemistry: techniques to generate molecular force via elongational flows. *Chem. Soc. Rev.* **2013**, *42*, 7497−7506.
(39) Lenhardt, J. M.; Ramirez, A. L. B.; Lee, B.; Kouznetsova, T. B.; Craig, S. L. Mechanistic Insights into the Sonochemical Activation of Multimechanophore Cyclopropanated Polybutadiene Polymers. *Macromolecules* **2015**, *48*, 6396−6403.
(40) McFadden, M. E.; Robb, M. J. Generation of an Elusive Permanent Merocyanine via a Unique Mechanochemical Reaction Pathway. *J. Am. Chem. Soc.* **2021**, *143*, 7925−7929.
(41) Osler, S. K.; McFadden, M. E.; Zeng, T.; Robb, M. J. Mechanochemical reactivity of a multimodal 2H-bis-naphthopyran mechanophore. *Polym. Chem.* **2023**, *14*, 2717−2723.
(42) McFadden, M. E.; Overholts, A. C.; Osler, S. K.; Robb, M. J. Validation of an Accurate and Expedient Initial Rates Method for Characterizing Mechanophore Reactivity. *ACS Macro Lett.* **2023**, *12*, 440−445.
(43) Overholts, A. C.; Robb, M. J. Examining the Impact of Relative Mechanophore Activity on the Selectivity of Ultrasound-Induced Mechanochemical Chain Scission. *ACS Macro Lett.* **2022**, *11*, 733−738.
(44) Lee, B.; Niu, Z.; Wang, J.; Slebodnick, C.; Craig, S. L. Relative Mechanical Strengths of Weak Bonds in Sonochemical Polymer Mechanochemistry. *J. Am. Chem. Soc.* **2015**, *137*, 10826−10832.
(45) Kucharski, T. J.; Huang, Z.; Yang, Q.; Tian, Y.; Rubin, N. C.; Concepcion, C. D.; Boulatov, R. Kinetics of Thiol/Disulfide Exchange Correlate Weakly with the Restoring Force in the Disulfide Moiety. *Angew. Chem., Int. Ed.* **2009**, *48*, 7040−7043.
(46) Groote, R.; Szyja, B. M.; Leibfarth, F. A.; Hawker, C. J.; Doltsinis, N. L.; Sijbesma, R. P. Strain-Induced Strengthening of the Weakest Link: The Importance of Intermediate Geometry for the Outcome of Mechanochemical Reactions. *Macromolecules* **2014**, *47*, 1187−1192.
(47) Ribas-Arino, J.; Shiga, M.; Marx, D. Understanding Covalent Mechanochemistry. *Angew. Chem., Int. Ed.* **2009**, *48*, 4190−4193.
(48) Sun, Y.; Kevlishvili, I.; Kouznetsova, T. B.; Burke, Z. P.; Craig, S. L.; Kulik, H. J.; Moore, J. S. The tension-activated carbon−carbon bond. *Chem.* **2024**, *10*, 3055−3066.
(49) O'Neill, R. T.; Boulatov, R. Experimental quantitation of molecular conditions responsible for flow-induced polymer mechanochemistry. *Nat. Chem.* **2023**, *15*, 1214−1223.
(50) Wang, J.; Kouznetsova, T. B.; Niu, Z.; Rheingold, A. L.; Craig, S. L. Accelerating a Mechanically Driven *anti* -Woodward−Hoffmann Ring Opening with a Polymer Lever Arm Effect. *J. Org. Chem.* **2015**, *80*, 11895−11898.
(51) Wang, Z.; Craig, S. L. Stereochemical effects on the mechanochemical scission of furan−maleimide Diels−Alder adducts. *Chem. Commun.* **2019**, *55*, 12263−12266.

https://doi.org/10.1021/jacs.4c18395
J. Am. Chem. Soc. 2025, 147, 3904−3911